20 May, 2014

Uitsluitend voor persoonlijk gebruik / for personal use only

**TU Delft Library**
Prometheusplein 1
Postbus 98
2600 MG Delft
Tel: +31 (0) 15 27 85678
Fax: +31 (0) 15 27 85706
Email: library@tudelft.nl
www.library.tudelft.nl

Aan: T.N.O.
CREDITEURENADMINISTRATIE

POSTBUS 6061
2600 JA DELFT

NEDERLAND

**Aanvraag nr: 1625890** Uw referentie(s): TS41021031 - H

**Artikelomschrijving:** Aantal kopieën: **6**

Artikel: DEEP-LEVEL TRANSIENT SPECTROSCOPY ON AN AMORPHOUS
Auteur: CHASIN
Titel: APPLIED PHYSICS LETTERS
Jaar: 2014 Vol. 104 Nr. 8 Pag. 082112
Plaatsnummer: 784 B

AIP | Applied Physics Letters

# Deep-level transient spectroscopy on an amorphous InGaZnO4 Schottky diode

Adrian Chasin, Eddy Simoen, Ajay Bhoolokam, Manoj Nag, Jan Genoe, Georges Gielen, and Paul Heremans

Citation: Applied Physics Letters **104**, 082112 (2014); doi: 10.1063/1.4867236
View online: http://dx.doi.org/10.1063/1.4867236
View Table of Contents: http://scitation.aip.org/content/aip/journal/apl/104/8?ver=pdfcov
Published by the AIP Publishing

**Articles you may be interested in**
Analysis of amorphous indium-gallium-zinc-oxide thin-film transistor contact metal using Pilling-Bedworth theory and a variable capacitance diode model
Appl. Phys. Lett. **102**, 152102 (2013); 10.1063/1.4801991

Determination of conduction band offset between strained CdSe and ZnSe layers using deep level transient spectroscopy
Appl. Phys. Lett. **100**, 252110 (2012); 10.1063/1.4729764

Operation mechanism of Schottky barrier nonvolatile memory with high conductivity InGaZnO active layer
Appl. Phys. Lett. **100**, 143502 (2012); 10.1063/1.3699221

Electron traps in amorphous In–Ga–Zn–O thin films studied by isothermal capacitance transient spectroscopy
Appl. Phys. Lett. **100**, 102106 (2012); 10.1063/1.3691923

Surface traps in vapor-phase-grown bulk ZnO studied by deep level transient spectroscopy
J. Appl. Phys. **104**, 063707 (2008); 10.1063/1.2978374

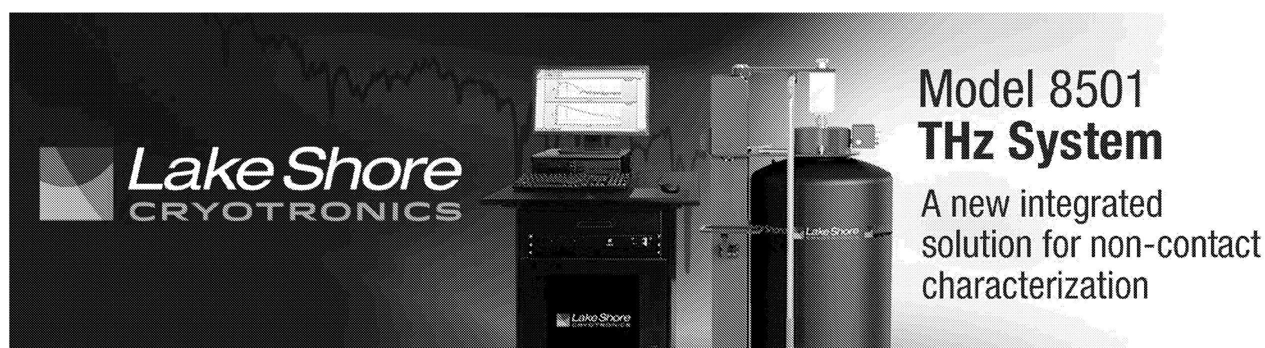


This article is copyrighted as indicated in the article. Reuse of AIP content is subject to the terms at: http://scitation.aip.org/termsconditions. Downloaded to IP: 131.180.130.218 On: Tue, 20 May 2014 13:04:21

APPLIED PHYSICS LETTERS **104**, 082112 (2014)

# Deep-level transient spectroscopy on an amorphous $InGaZnO_4$ Schottky diode

Adrian Chasin,[1,2,a] Eddy Simoen,[1,3] Ajay Bhoolokam,[1,2] Manoj Nag,[1,2] Jan Genoe,[1,2] Georges Gielen,[2] and Paul Heremans[1,2]
[1]*imec, Kapeldreef 75, 3001 Leuven, Belgium*
[2]*ESAT, KU Leuven, Kasteelpark Arenberg 10, 3001 Leuven, Belgium*
[3]*Department of Solid State Sciences, Ghent University, Krijgslaan 281-S1, 9000 Gent, Belgium*

(Received 27 January 2014; accepted 17 February 2014; published online 27 February 2014)

The first direct measurement is reported of the bulk density of deep states in amorphous IGZO (indium-gallium-zinc oxide) semiconductor by means of deep-level transient spectroscopy (DLTS). The device under test is a Schottky diode of amorphous IGZO semiconductor on a palladium (Pd) Schottky-barrier electrode and with a molybdenum (Mo) Ohmic contact at the top. The DLTS technique allows to independently measure the energy and spatial distribution of subgap states in the IGZO thin film. The subgap trap concentration has a double exponential distribution as a function energy, with a value of $\sim 10^{19}\,cm^{-3}\,eV^{-1}$ at the conduction band edge and a value of $\sim 10^{17}\,cm^{-3}\,eV^{-1}$ at an energy of 0.55 eV below the conduction band. Such spectral distribution, however, is not uniform through the semiconductor film. The spatial distribution of subgap states correlates well with the background doping density distribution in the semiconductor, which increases towards the Ohmic Mo contact, suggesting that these two properties share the same physical origin. © *2014 AIP Publishing LLC*. [http://dx.doi.org/10.1063/1.4867236]

Amorphous oxide semiconductors (AOS) are considered prime candidates as channel material for thin-film transistors for display backplanes because of their superior charge carrier mobility compared to amorphous silicon or to organic semiconductors, combined with their low-temperature processability. Among different candidates, IGZO (indium-gallium-zinc oxide) has attracted most of the attention, mainly due to its chemical stability and easy processability.[1] However, being amorphous, IGZO has intrinsically a high concentration of subgap states. Depending on their energy level, these states have distinct negative impacts on the Thin-Film Transistor (TFT) performance, to cite a few: deterioration of the subthreshold slope,[2] shift of the threshold voltage,[3] reduction of the mobility,[4] and bias-stress instability.[3,5]

Even though significant work has been devoted to modeling and understanding of the charge trapping and related instability, until now all the experimental characterizations were based on I-V and C-V measurements on MIS[6] or TFT structures.[7–9] In field-effect and C-V measurements one changes the bias voltage, which simultaneously varies both the width of the space-charge layer and the intersection of the Fermi level with the density of states. The data are thus a convolution of the energy and spatial variation in gap states. All analyses of these data have assumed that the states are distributed uniformly in space. By applying Deep Level Transient Spectroscopy (DLTS) measurements on Schottky diodes, it is possible to separate the spatial and energy measurements.[10] The energy is measured by observing the thermal emission of carriers initially trapped in the subgap states while the spatial variation can be independently measured by simply changing the bias voltage applied to the sample.

[a]Author to whom correspondence should be addressed. Electronic mail: adrian.chasin@imec.be. Tel.: +32 6 28 83 97.

In conventional crystalline semiconductors with a discrete trap energy level and a well-defined activation energy, the DLTS signal as a function of temperature goes through a maximum ($\tau_{max}$) at the temperature where the transient time constant of the emitted charge carrier is on the order of the time-gate spacing used to obtain the DLTS signal. By using different gate spacing and plotting $\tau_{max}$ in an Arrhenius plot, the energy level $E_t$ of the trap and its capture cross section $\sigma_n$ can be extracted. On the other hand, the concentrations of deep levels in the discrete defect case are related to the respective magnitude of the peaks in the DLTS spectrum.[10] In the case of a disordered amorphous semiconductor, however, the DLTS spectrum is broad and rather featureless. In this case, the DLTS signal is simply an unresolved superposition of DLTS sharp lines originated from each trap level with a weighting function that is proportional to the trap concentration distribution over the various possible energies (the density of states function). Thus, if the trap levels are completely saturated after the filling pulse, the DLTS signal represents the subgap DOS (Density of States) multiplied by the temperature.

The trap energy level cannot be therefore measured from an Arrhenius plot, but it is calculated from the electron thermal-emission rate relation

$$E_c - E_t = kTln(\sigma_n v_{th} N_c \tau_0), \quad (1)$$

where kT is the thermal energy, $\sigma_n$ is the electron capture cross section of the trap, $v_{th}$ is the electron thermal velocity, $N_c$ is the available states in the conduction band, and $\tau_0$ is the emission rate window. In this work, $\sigma_n$ is assumed to be $10^{-15}\,cm^2$ and independent of the temperature. The available number of states in the conduction band, which is temperature dependent, is calculated using $m^* = 0.34 m_e$,[11] the thermal velocity of electrons in the semiconductor is calculated

 © 2014 AIP Publishing LLC

This article is copyrighted as indicated in the article. Reuse of AIP content is subject to the terms at: http://scitation.aip.org/termsconditions. Downloaded to IP: 131.180.130.218 On: Tue, 20 May 2014 13:04:21

using the standard equation $v_{th} = \sqrt{3kT/m^*}$ and the rate window $\tau_0$ is approximated to be half of the time window $t_w$ used in the measurements ($t_w = 51.2$ ms).

On the other hand, as briefly discussed before, the concentration of the various deep levels $N_t$ can be directly related to the respective magnitudes of the DLTS spectrum ($\Delta$C). In this case, $\Delta$C indicates the ratio of the deep-level trap concentration to the uncompensated shallow-level concentration in the depletion region $N_{depl}$

$$N_t = \frac{N_{depl}}{2}\frac{\Delta C}{C}\frac{1}{kT} \quad (\text{in}\,\text{cm}^{-3}\text{eV}^{-1}). \tag{2}$$

Therefore, $N_{depl}$ must be measured in order to determine $N_t$. The value of $N_{depl}$ can be obtained from C-V measurements via the well-known relation

$$\frac{A^2}{C^2} = \left(\frac{2}{\varepsilon_S \varepsilon_0 N_{depl}}\right)\left(V_{bi} - \frac{kT}{q} - V\right), \tag{3}$$

showing that $N_{depl}$ can be determined from the slope of $A^2/C^2$ as a function of the applied bias on the Schottky diode. In Eq. (3), $V_{bi}$, the diodes's built-in potential, is found as the intersection of the curve with the voltage axis. Further, $\varepsilon_S$ is the static dielectric constant of the semiconductor, being equal to 13.9 (Ref. 12) and $\varepsilon_0$ is the dielectric constant of vacuum.

The main reason for using a Schottky diode to extract the semiconductor subgap DOS is the device simplicity: the raw DLTS spectrum already roughly indicates the subgap DOS shape and distribution.[13] Moreover, the subgap DOS can be easily calculated using the equations and assumptions described previously, without the need for numerical iterative calculations that can add cumulative errors in the final obtained subgap DOS. The fabrication of near-ideal IGZO Schottky diodes with large rectification ratio is not straightforward and involves metal and IGZO thickness optimization.[12,14,15] The device is based on a vertical structure as shown in the inset of Fig. 1(b). The bottom contact is 30 nm Pd, which forms the Schottky contact to the a-IGZO. Afterwards, a 100 nm thick amorphous IGZO layer was deposited by RF sputtering from an $InGaZnO_4$ ceramic target at room temperature. The oxygen content of the ($Ar + O_2$) gases was maintained at 20% and the working pressure in the deposition chamber was $2 \times 10^{-2}$ mbar. The IGZO layer was wet etched in a solution of oxalic acid and water and annealed at 200 °C for 1 h in an oxygen environment. As a final step, Ohmic Mo top contacts were formed by a lift-off process, providing vertical diodes with area of $15 \times 5\,\mu m^2$ to $220 \times 200\,\mu m^2$. All the DLTS related experiments shown here were performed on the $220 \times 200\,\mu m^2$ diode.

The I-V curves of the fabricated are shown in Figure 1(a). It is clear that the diode current is directly proportional to its area, increasing exponentially as a function of the applied bias, which indicates that the diode charge transport mechanism can be modeled by thermionic emission given by

$$I = AA^*T^2 \exp\left(\frac{-q\Phi_B}{kT}\right)\left\{\exp\left[\frac{q(V - IR_S)}{nkT}\right] - 1\right\}, \tag{4}$$

where A* is the effective Richardson constant, which for IGZO has a theoretical value of $41\,\text{A}\,\text{cm}^{-2}\,\text{K}^{-2}$, A is the area of the diode, and $R_S$ is its series resistance. All the diodes have a small ideality factor $n$ equal to 1.2 and rectification ratios higher than $10^7$ at $\pm 1$ V, which means a Schottky barrier height $\Phi_B$ of 0.8 eV. Figure 1(b) shows the background doping concentration $N_{depl}$ calculated from Eq. (3) as a function of the depletion region thickness W. It is clear that $N_{depl}$ is not spatially constant within the IGZO film, but it increases in the direction of the film top surface (ohmic contact).

In order to accurately extract the IGZO subgap DOS, two pre-requisites have to be fulfilled during the DLTS measurements. First, the Schottky diode cannot be frozen-in. As IGZO has a relatively low electron mobility compared to traditional crystalline semiconductors, it is possible that the combination of high-frequency C-V measurements (1 MHz for the DLTS set-up) with the low temperature causes the semiconductor to become an insulator, not responding anymore to the applied bias. Second, the subgap traps have to be completely filled after the filling voltage pulse, which means that the DLTS signal has to be saturated by a sufficiently long pulse. If these two conditions are fulfilled, Eq. (2) can be directly correlated to subgap DOS density.

Figure 2(a) shows the capacitance density as a function of the reverse bias for different temperatures. All curves show the expected voltage dependency of a Schottky capacitance junction, indicating that the semiconductor is not frozen-in and can respond to the applied ac voltage at 1 MHz, even at low temperatures. Indeed, as shown in the

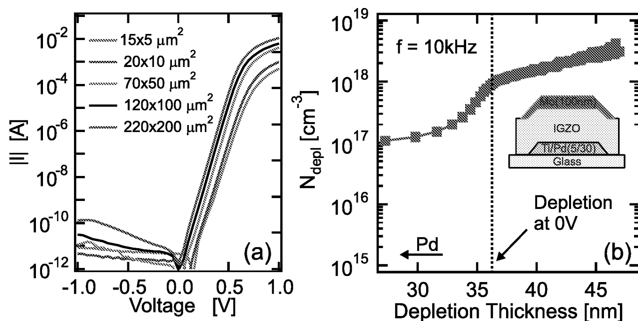


FIG. 1. (a) I-V curves of the vertical a-IGZO Schottky diodes with different areas and (b) the corresponding background doping density as a function of the depletion region thickness. Both measurements were performed at room temperature. The IGZO layer has a thickness of 100 nm.

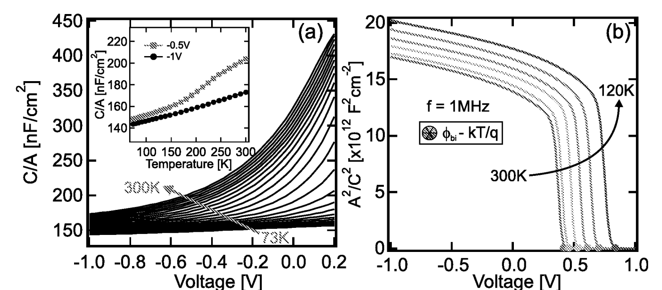


FIG. 2. (a) CV curves of the IGZO Schottky diode as a function of the reverse bias at different temperatures. The inset shows the value of the diode's capacitance as a function of the temperature at two different reverse biases. (b) CV measurement, revealing the diode's built-in voltage temperature dependency.

This article is copyrighted as indicated in the article. Reuse of AIP content is subject to the terms at: http://scitation.aip.org/termsconditions. Downloaded to IP: 131.180.130.218 On: Tue, 20 May 2014 13:04:21

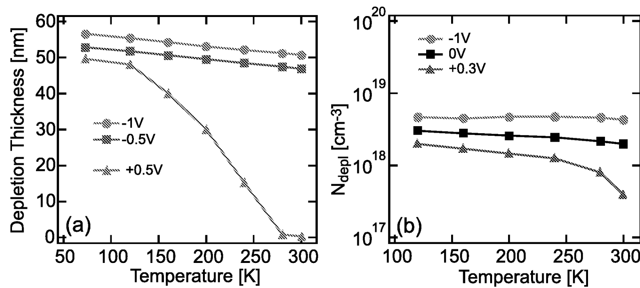


FIG. 3. (a) The depletion region thickness and the (b) background doping density as a function of the temperature and biases.

inset of Figure 2(a), the capacitance of the diode increases as a function of the temperature, which is caused by the diode's built-in voltage dependency on the temperature. The decrease of $V_{bi}$ as a function of the temperature is clearly shown in Figure 2(b), where $V_{bi}$ is extracted at the intersection of the $A^2/C^2$ curve with the voltage axis. At room temperature, $V_{bi}$ is equal to 0.42 V, while at 120 K it increases to a value of 0.82 V. The increase of the diode's built-in voltage has a direct impact on the diode's depletion region, especially for forward biases as shown in Figure 3(a) for three different biases. For a forward bias of 0.5 V, which is about the diode's $V_{bi}$ at room temperature, the depletion region is negligibly small. However, due to the increase of the diode's built-in voltage at low temperatures and the specific spatial doping concentration in the IGZO film, the depletion region is much larger at 70 K for the same applied bias of 0.5 V.

As indicated by Eq. (2), the doping concentration of the IGZO film $N_{depl}$ must be carefully measured as a function of the temperature. Figure 3(b) shows $N_{depl}$ as a function of the temperature for three different biases. It is clear that even though $N_{depl}$ shows a dependency on the applied voltage, as already previously observed in Figure 1(b), $N_{depl}$ is almost constant as a function of temperature for the same applied bias.

Figure 4(a) shows the DLTS signal as a function of the filling pulse time for two different pulse voltages at room temperature. First, it shows that in IGZO the dynamic trap filling phenomena do not follow an exponential function as shown by the dashed line, but a much slower logarithmic dependency on the filling pulse duration. Such capture kinetics was previously observed for dislocations in crystalline semiconductors[16] and can be explained by the distribution of the deep levels in a-IGZO. Such a distribution of defects can

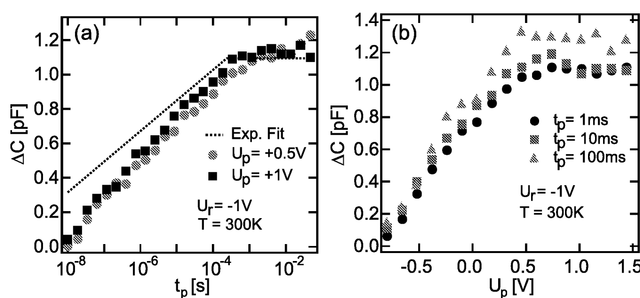


FIG. 4. (a) Capture kinetics of electron trapping for two different filling pulse voltages and (b) the magnitude of the DLTS spectrum as a function of the filling pulse voltage. Both measurements were performed at room temperature.

accommodate multiple charge carriers during the trapping process, which leads to a non-exponential dependency of the trap filling on the filling pulse time. As a consequence it is not possible to extract the electron capture cross-section, in contrast to the situation for a single discrete trap level with a classical exponential capture kinetics. For this reason, $\sigma_n$ is assumed to be a constant value of $10^{-15}\,cm^2$ which corresponds with a typical value for a neutral deep-level center. Figure 4(a) also shows that the DLTS signal saturates at $t_p \sim 10\,ms$, which reveals the minimum filling time pulse width to be used in order to correctly extract the IGZO subgap DOS. Figure 4(b) shows the DLTS signal as a function of the filling pulse amplitude for three different filling times at room temperature. The DLTS signal saturates once more at a value of $U_p \sim +0.5\,V$, which is therefore used during the DLTS measurements.

Having fulfilled the two requirements for the correct measurement of the subgap DOS, it is possible to proceed to the DLTS measurements itself. Figure 5(a) shows the DLTS spectrum obtained at a reverse bias of 1 V, for a saturating filling pulse voltage of +0.5 V and for four different filling pulse times. As expected for an amorphous semiconductor, the DLTS signal is featureless with no clear and sharp peaks. Moreover, ΔC increases as a function of the filling pulse time, revealing a saturation for $t_p \sim 10\,ms$, as previously observed in Figure 4(a). The subgap DOS is calculated using Eq. (2) and plotted as a function of the energy from the band mobility edge, as shown by the black curve in Figure 5(b). These measurements reveal two interesting regimes: an exponential distribution of traps from the conduction band edge $E_c$ to 0.2 eV below $E_c$; and a second exponential distribution with a higher characteristic energy at $E_c$-$E_t > 0.3\,eV$. However, due to the strong influence of the temperature on the diode's built-in voltage, this curve is not quantitatively accurate. During the DLTS measurements, one fills the traps in the spatial interval $W_r - W_p$, corresponding to the reverse and filling bias $V_r$ and $V_p$, respectively. In this way, only the traps in the fraction $(W_r - W_p)/W_r$ of the total depletion width contribute to the DLTS signal ΔC. If the depletion region at the filling pulse varies as a function of the temperature, the calculated trap distribution $N_t$ must be multiplied by a correction factor equal to $[W_r/(W_r - W_p)]$ in order to obtain the right trap distribution, and consequently the subgap DOS value. Both the correction factor and the final subgap DOS distribution are shown in Figure 5(b). As noticed before, it reveals two exponential distributions at $E_c$-$E_t < 0.2\,eV$ and $E_c$-$E_t > 0.3\,eV$ with characteristic energies of 80 meV ($E_{01}$) and 227 meV ($E_{02}$), respectively. The first exponential distribution, which corresponds to the IGZO tail states, intersects the conduction mobility edge at $1.6 \times 10^{19}\,cm^{-3}\,eV^{-1}$. This value is at least two orders of magnitude lower than for conventional hydrogenated amorphous silicon (a-Si:H).[17] Our results agree well with some proposed models that indicate a double exponential distribution of subgap DOS in IGZO,[5,18] in contrast to a-Si:H that presents also a Gaussian subgap DOS.[17] These measurements can discard the influence of interface traps as they were performed within regions 50 nm away from the interfaces of the 100 nm IGZO thick film. Moreover, as we are using a simple Schottky diode, there are no interface states

This article is copyrighted as indicated in the article. Reuse of AIP content is subject to the terms at: http://scitation.aip.org/termsconditions. Downloaded to IP: 131.180.130.218 On: Tue, 20 May 2014 13:04:21

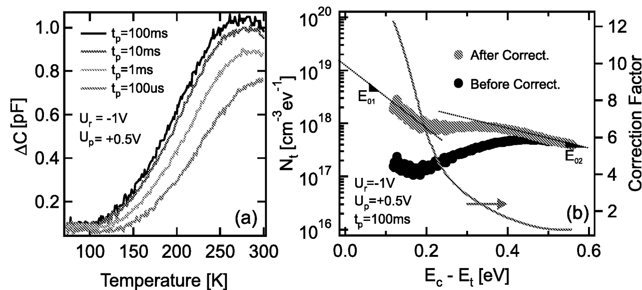


FIG. 5. (a) DLTS spectrum for four different filling pulse times and (b) the correspondent subgap DOS, calculated using the DLTS spectrum with $t_p = 100$ ms.

arising from dielectrics present in other more complex structures such as MIS or TFTs devices. It should also be mentioned that our assumption for $\sigma_n$ does not have any impact on the extracted exponentials characteristic energies and has only a small influence on the DOS distribution energy level itself. If $\sigma_n$ is changed by one order of magnitude, for example, the $N_t$ curve is shifted by only 40 meV.

The measurements shown in Figure 5 were obtained at a reverse bias of 1 V, which corresponds to a large depletion region thickness of 52 nm at room temperature. If the same measurements are performed, however, at other reverse biases, corresponding to different spatial regions within the IGZO film, the results are not the same. Figure 6(a) shows that the DLTS spectrum magnitude is larger for smaller reverse bias voltages, or in other words, it is larger for smaller voltage pulses ($U_p$-$U_r$). Such behavior, however, does not indicate a higher defect concentration as it is clear from Figure 6(b), which shows once more the corrected subgap DOS as a function of the energy, calculated using Eqs. (1) and (2), respectively. For smaller reverse biases, the larger magnitude of the DLTS signal is mainly due to the larger capacitance value, and the resulting $N_t$ is actually smaller than the one at larger reverse biases. This means that in the regions closer to the IGZO top-surface, the subgap DOS is larger than in the depleted regions next to the Schottky junction. It also shows that the slope of the exponential tail state is larger closer to the Schottky junction, while the second exponential at higher energies has a constant characteristic energy throughout the IGZO film. Our measurements also allow us to compare the background doping density and the IGZO subgap DOS at a specific energy as a function of the depletion region thickness. This is shown in Figure 7, for the trap density at $E_c$-$E_t$ = 0.55 eV. This

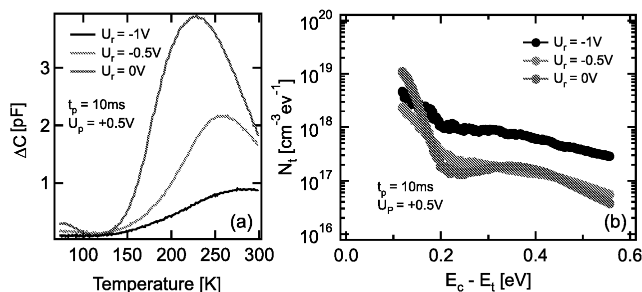


FIG. 6. (a) DLTS spectrum dependency on the reverse bias and (b) the correspondent subgap DOS for the three different reverse bias voltages.

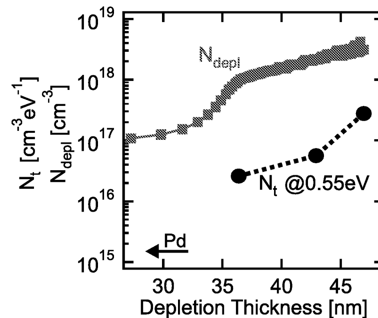


FIG. 7. The background doping density and the subgap DOS at $E_c$-$E_t$ = 0.55 eV as a function of the IGZO depletion region thickness.

energy corresponds to the room temperature measurement, in which the filling pulse amplitude guarantees that all traps are filled within the depletion region. Such condition allows us to determine the effective depletion depth value that corresponds to each reverse applied bias. There is a remarkable similarity between the doping concentration and trap distribution, suggesting that these properties share the same physical origin. X-ray photoelectron spectroscopy (HX-PES) in highly doped amorphous In-Zn-O (Ref. 19) indicated that near conduction band minimum (CBM) states can be attributed to donor electrons. However, in the case of IGZO, the highly doped region next to the film top surface cannot be linked to free electrons in the semiconductor conduction band, but it is the contribution of effective shallow donor and subgap deep acceptor states.

In conclusion, by combining the DLTS technique with Schottky diodes, we have been able to directly measure the subgap density of states of amorphous indium-gallium-zinc oxide semiconductor. First, the parameters to assure the correct DOS measurement, such as the filling pulse time duration and the voltage have been carefully analyzed. Afterwards, based on these variables and taking in to account the strong built-in voltage dependency of the IGZO diode on the temperature, it was possible to analytically extract the subgap DOS distribution. It revealed a double exponential dependency on the energy, with characteristic energies of 80 meV and 226 meV, for $E_c$-$E_t < 0.2$ eV (the tail states) and $E_c$-$E_t > 0.3$ eV (deep levels), respectively. Moreover, we have shown that the DLTS spectrum and the background doping density are correlated, confirming that the measured background doping density is a result from both effective electron doping and acceptor electron subgap levels.

The research leading to these results received funding from the European Community's Seventh Framework Program FP7-ICT-2009-4 under Grant Agreement No. 247798 of the ORICLA project. We appreciated very much the help of Dr. Johan Lauwaert (University of Ghent) in setting up the DLTS experiments.

[1]K. Nomura, H. Ohta, A. Takagi, T. Kamiya, M. Hirano, and H. Hosono, Nature **432**, 488 (2004).
[2]H.-H. Hsieh, T. Kamiya, K. Nomura, H. Hosono, and C.-C. Wu, Appl. Phys. Lett. **92**, 133503 (2008).
[3]K. Nomura, T. Kamiya, M. Hirano, and H. Hosono, Appl. Phys. Lett. **95**, 013502 (2009).
[4]K. Hoshino, D. Hong, H. Q. Chiang, and J. F. Wager, IEEE Trans. Electron Devices **56**, 1365 (2009).

This article is copyrighted as indicated in the article. Reuse of AIP content is subject to the terms at: http://scitation.aip.org/termsconditions. Downloaded to IP: 131.180.130.218 On: Tue, 20 May 2014 13:04:21

[5]E. N. Cho, E. N. Cho, J. H. Kang, C. E. Kim, P. Moon, and I. Yun, IEEE Trans. Device Mater. Reliab. **11**, 112 (2011).
[6]K. Hayashi, A. Hino, S. Morita, S. Yasuno, H. Okada, and T. Kugimiya, Appl. Phys. Lett. **100**, 102106 (2012).
[7]H. Bae, H. Choi, S. Oh, D. H. Kim, J. Bae, J. Kim, Y. H. Kim, and D. M. Kim, IEEE Electron Devices Lett. **34**, 57 (2013).
[8]S. Lee, S. Park, S. Kim, Y. Jeon, K. Jeon, J.-H. Park, J. Park, I. Song, C. J. Kim, Y. Park, D. M. Kim, and D. H. Kim, IEEE Electron Devices Lett. **31**, 231 (2010).
[9]M. Kimura, T. Nakanishi, K. Nomura, T. Kamiya, and H. Hosono, Appl. Phys. Lett. **92**, 133512 (2008).
[10]D. V. Lang, J. Appl. Phys. **45**, 3023 (1974).
[11]A. Takagi, K. Nomura, H. Ohta, T. Kamiya, M. Hirano, and H. Hosono, Thin Solid Films **486**, 38 (2005).
[12]D. H. Lee, K. Nomura, T. Kamiya, and H. Hosono, IEEE Electron Devices Lett. **32**, 1695 (2011).
[13]D. V. Lang, J. D. Cohen, and J. P. Harbison, Phys. Rev. B **25**, 5285 (1982).
[14]A. Chasin, S. Steudel, K. Myny, M. Nag, T.-H. Ke, S. Schols, J. Genoe, G. Gielen, and P. Heremans, Appl. Phys. Lett. **101**, 113505-1 (2012).
[15]A. Chasin, M. Nag, A. Bhoolokam, K. Myny, S. Steudel, S. Schols, J. Genoe, G. Gielen, and P. Heremans, IEEE Trans. Electron Devices **60**, 3407 (2013).
[16]C. Nyamhere, F. Cristiano, F. Olivie, Z. Essa, E. Bedel-Pereira, D. Bolze, and Y. Yamamoto, J. Appl. Phys. **113**, 184508 (2013).
[17]R. A. Street, *Technology and Applications of Amorphous Silicon* (Springer, Berlin, 2000).
[18]K. Jeon, C. Kim, I. Song, J. Park, S. Kim, S. Kim, Y. Park, J.-H. Park, S. Lee, D. M. Kim, and D. H. Kim, Appl. Phys. Lett. **93**, 182102 (2008).
[19]T. Shibuya, M. Yoshinaka, Y. Shimane, F. Utsuno, K. Yano, K. Inoue, E. Ikenaga, J. J. Kim, S. Ueda, M. Obata, and K. Kobayashi, Thin Solid Films **518**, 3008 (2010).

This article is copyrighted as indicated in the article. Reuse of AIP content is subject to the terms at: http://scitation.aip.org/termsconditions. Downloaded to IP: 131.180.130.218 On: Tue, 20 May 2014 13:04:21